Femtosecond Spectral Holography

Andrew M. Weiner, *Senior Member, IEEE,* Daniel E. Leaird, David H. Reitze, and Eung Gi Paek

Invited Paper

***Abstract*—Storage, recall, and processing of shaped femtosecond waveforms are achieved by performing spectral holography within a femtosecond pulse shaping apparatus. Time reversal, as well as correlation and convolution, of femtosecond temporal signals are demonstrated. Applications of this technique to matched filtering, dispersion compensation, encryption and decoding, and femtosecond waveform synthesis are also discussed. Our work extends the powerful principles of holographic signal processing, which have been used extensively for pattern recognition and filtering of two-dimensional spatial signals, to the femtosecond time domain.**

I. Introduction

TEMPORAL shaping of ultrashort light pulses was previously achieved by phase and amplitude filtering of optical frequency components spatially dispersed within a simple grating and lens assembly [1]–[5]. By means of this technique, femtosecond pulse waveforms were specially synthesized for studies involving pulse coding for spread spectrum communications, [3], [6] dark soliton propagation in fibers, [7] all-optical switching, [8] fiber dispersion compensation, [9] measurement of ultrashort pulse shapes, [10] and ultrafast spectroscopy [11]. Other related pulse shaping techniques have also been reported [12]–[16] and applied [15], [17]. In all of these methods, pulse shaping is accomplished by linear filtering of the individual optical frequencies which compose incident ultrashort pulses. Thus, given knowledge of the input pulse, a specified output waveform can be generated by implementing the appropriate linear filter.

Despite the power of these techniques, certain basic signal processing operations, such as time reversal, correlation, and convolution of independently varying waveforms, cannot be performed by means of linear filtering. Similarly, if the input pulse is not specified, then the linear filter needed to produce a desired output cannot be calculated. Operations such as these require nonlinear filtering. In this paper we demonstrate a frequency domain holographic processing technique which allows nonlinear filtering, time reversal, correlation, and convolution of femtosecond pulse waveforms. Holographic techniques have been widely used in the spatial domain for storage and recall of images and to perform signal processing operations such as correlations for pattern recognition applications [18]. Our aim is to harness the powerful principles of holographic signal processing for the use in the ultrafast time domain.

Manuscript received March 25, 1992; revised June 18, 1992.
The authors are with Bellcore, Red Bank, NJ 07701-7040.
IEEE Log Number 9202606.

Several techniques have been put forth for storage, recall, and processing of ultrafast optical waveforms. The use of degenerate four-wave mixing to achieve time-reversal of amplitude- (but not phase-) modulated pulses has been proposed, [19] but to our knowledge has not yet been tested. Several workers have demonstrated storage and processing of optical pulses via spectral hole burning and photon echoes in inhomogeneously broadened resonant absorbers, which are usually held at cryogenic temperatures [20]–[25]. In some cases femtosecond operation has been achieved [23], [24]. This technique requires that the laser wavelength coincide with the absorption line and is subject to some restrictions imposed by causality. A full discussion of pulse processing via photon echoes and its relation to spectral holography is given in the article by Silberberg in this issue [26]. Finally, some simple examples of storage and recall of femtosecond pulses using time domain holography were recently reported [27], [28].

Storage and reconstruction of shaped ultrafast waveforms by holographic recording of spatially dispersed optical frequency components was proposed by Mazurenko [29]. Unlike the photon echo method, this technique can utilize spectrally nonselective media, does not require cryogenic temperatures, and is not subject to the same causality conditions. In this paper we report such holographic storage and read out of shaped femtosecond pulses, which we achieve by performing spectral holography within a femtosecond pulse shaping apparatus [30]. Our results demonstrate time reversal and processing, as well as storage and subsequent read out, of femtosecond optical waveforms.

The body of this paper is structured as follows. In Section II we discuss the experimental setup and the basic principles. Section III describes the experimental results. In addition to time reversal, correlation, and convolution operations, additional operations, such as matched filtering of femtosecond waveforms, encrypted femtosecond data storage, and femtosecond waveform synthesis, are also demonstrated. Further discussion and indications of further applications are included in Section IV. In Section V we conclude.

II. Experimental Setup

Femtosecond spectral holography may be considered a temporal analog of traditional spatial-domain Fourier-transform holography. In traditional holography information on a spatially patterned signal beam is recorded as a set of fringes arising due to interference with a spatially

uniform reference beam. Subsequent illumination of the hologram with a uniform test (or read out) beam reconstructs either a real or conjugate image of the original signal beam, depending on the geometry. In our time domain work, the reference is a short pulse with a broad and regular spectrum. The signal is a shaped pulse with information patterned onto the spectrum. During holographic recording the complex amplitude of each signal pulse spectral component is stored as a series of fringes arising due to interference with the corresponding spectral component from the reference pulse. Subsequent illumination with a short test pulse produces either a real or a time-reversed (conjugate) replica of the original signal pulse, again depending on the geometry. Illumination with a temporally shaped pulse results either in the correlation or the convolution of the test and signal waveforms, again in analogy with traditional, spatial domain holography.

Our spectral holography setup is shown schematically in Fig. 1 [30]. The basic layout is identical to the arrangement used previously for shaping of femtosecond pulses [5]. The apparatus consists of a pair of diffraction gratings placed at the outside focal planes of a unit-magnification confocal lens pair. The first grating and lens spatially disperse the individual optical frequency components contained within incident femtosecond pulses (along a direction we denote as x). Maximum spectral resolution is obtained at the plane midway between the lens pair. In the conventional pulse shaping apparatus described in our previous work, a patterned mask [5] or a multielement modulator array [31], [32] was placed in this plane in order to control the phases and amplitudes of the spatially dispersed frequency components. After the second lens and grating recombined the individual frequencies into a single collimated beam, the output pulse shape was given by the Fourier transform of the pattern transferred from the mask onto the spectrum. In the current paper the prepatterned mask is replaced by a thin holographic medium; and in order to record a spectral hologram [Fig. 1(a)] two beams, a shaped signal pulse and a short reference pulse, are incident onto the apparatus. Prior to the pulse shaper, reference and signal beams are set for parallel but noncollinear propagation, with zero relative time delay. The first grating and lens spread frequency components from both beams along x. The lens causes the spectrally dispersed reference and signal beams to intersect on the holographic plate, forming interference fringes along the y direction. Recording these fringes in the holographic medium forms a spectral hologram, in which the amplitude and phase of each spectral component of the incident signal beam is encoded in terms of the amplitude and spatial phase of the grating present at the corresponding position along x.

After recording, spectral holograms were read out by using a single test beam [Fig. 1(b)]. The individual frequency components of the test beam are first spread spatially and then impinge on the spectral hologram. Each spectral component diffracts off that part of the hologram containing phase and amplitude information corresponding to the same frequency component from the signal beam. All the diffracted frequencies are then recombined into a single beam; at this point the reconstructed field $E_{\text{out}}(\omega)$ can be written roughly as follows:

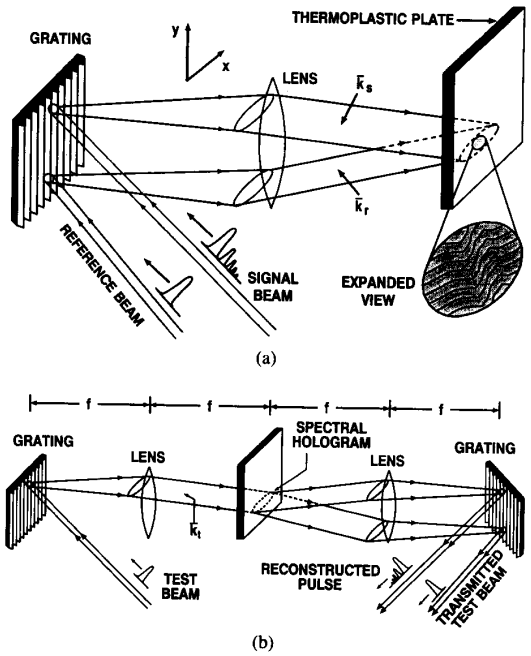

Fig. 1. Schematic illustration of the apparatus for femtosecond spectral holography. (a) Setup for recording the spectral hologram. Only the front half of the pulse shaping apparatus is shown. The expanded view of the spectral hologram illustrates one possible interference pattern between spectrally dispersed signal and reference beams. (b) Setup for reading out the spectral hologram.

$$E_{\text{out}}(\omega) \sim E_t(\omega)E_r^*(\omega)E_s(\omega)e^{i\bar{K}_1\cdot\bar{r}} + E_t(\omega)E_r(\omega)E_s^*(\omega)e^{i\bar{K}_2\cdot\bar{r}} \quad (1)$$

where

$$\bar{K}_1 = \bar{k}_t - \bar{k}_r + \bar{k}_s$$

and

$$\bar{K}_2 = \bar{k}_t + \bar{k}_r - \bar{k}_s.$$

Here $E_t(\omega)$, $E_r(\omega)$, and $E_s(\omega)$ are the complex spectral amplitudes of the test, reference, and signal fields, respectively, and $\bar{k}_t$, $\bar{k}_r$, and $\bar{k}_s$ are the propagation vectors of these beams just prior to the hologram. Equation (1) assumes that the recording is linearly proportional to exposure and neglects effects due to the finite spectral resolution of the pulse shaping apparatus. Because a thin holographic medium is used, Bragg matching is not required, and diffraction occurs in both the $\bar{K}_1$ and $\bar{K}_2$ directions. The envelopes of the reconstructed output pulses are given by the Fourier transform of (1), as follows:

$$e_{\text{out}}(t) \sim e_t(t) * e_r(-t) * e_s(t)e^{i\bar{K}_1\cdot\bar{r}} + e_t(t) * e_r(t) * e_s(-t)e^{i\bar{K}_2\cdot\bar{r}} \quad (2)$$

where $e_{out}(t)$, $e_t(t)$, $e_r(t)$, and $e_s(t)$ are the complex electric field amplitudes of the output, test, reference, and signal beams, respectively, and the * sign denotes convolution. When both test and reference beams consist of unshaped pulses with durations short compared to the duration of the shaped signal pulse, the first term in (2) represents a real reconstructed signal pulse ($e_{out}(t) \sim e_s(t)$), emerging from the hologram in the $\bar{K}_1$ direction, whereas the second term signifies a time-reversed reconstruction ($e_{out}(t) \sim e_s(-t)$), propagating along $\bar{K}_2$. In both cases the sharpest temporal features of the original signal pulse may be blurred due to the convolution with test and reference pulses. Furthermore, if the test beam itself consists of a shaped pulse, then in the $\bar{K}_1$ direction the reconstructed output waveform is given by the convolution of test and signal waveforms, while in the $\bar{K}_2$ direction the reconstructed pulse is equal to the correlation of test and signal waveforms. Note that these convolution and correlation operations involve electric field amplitudes, as opposed to intensity correlations commonly measured, e.g., by second harmonic generation.

The overall experimental setup is sketched in Fig. 2. Input pulses, typically 75 fs in duration at a 0.62 μm wavelength and a 120 MHz repetition rate, were obtained from a colliding-pulse mode-locked (CPM) dye laser [33]. The reference pulse is taken directly from the CPM laser; the signal beam is temporally shaped by spectral masking in a second, auxiliary pulse shaping apparatus. A 128 element liquid crystal phase modulator within the second pulse shaper makes possible reconfiguration of the signal waveform under computer control [32]. A stepper motor driven translation stage is used to adjust the relative delay between reference and signal beams at the input to the holographic shaping apparatus (usually the delay is set to zero). The holographic shaper consists of a pair of 600-line/mm gratings placed at the outside focal planes of a pair of 50 mm focal length, f1.4 camera lenses. A thermoplastic plate [34] placed midway between the lenses serves as a thin holographic medium. The spectral dispersion of the holographic shaping apparatus is given by $\delta x/\delta\lambda = f/d \cos\theta_d$, where f, d, and θ_d are the focal length, grating period, and diffracted angle, respectively. Experimentally $\theta_d = 60°$ and $\delta x/\delta\lambda = 0.06$ mm/nm. The spectrally dispersed reference and signal beams intersect on the thermoplastic plate, making a full crossing angle of 20° in the y direction in order to match the spatial frequency response of the thermoplastic plate. The intersection region extends ~ 0.6 mm along x (for a typical 10 nm bandwidth) and ~ 27 μm along y. Holograms were written on the thermoplastic plate using a Newport Corp. Model HC-3000 holographic recording system. Exposures energies were on the order of 4 nJ total (split 1.6:1 between reference and signal), corresponding to a fluence of $\sim 2.4 \times 10^{-5}$ J/cm^2 in a 4 ms exposure time. The diffraction efficiency was typically in the vicinity of 10%.

For read out we reused either the original reference or signal beam as the test beam. The beam not used as the test is blocked during read out. When the test beam is collinear with the original reference ($\bar{k}_t = \bar{k}_r$), we look at the real reconstructed beam emerging along $\bar{k}_s$; the other diffracted beam along $2\bar{k}_r - \bar{k}_s$ misses the second camera lens and is lost. Similarly, when $\bar{k}_t = \bar{k}_s$, we examine the time-reversed diffracted beam along $\bar{k}_r$. Note that the liquid crystal modulator used to control the signal waveform can be reprogrammed before read out. Thus, a test beam along $\bar{k}_s$ can be set to the original signal waveform, to a short 75 fs pulse, or to a new and different waveform. The temporal profiles of the reconstructed waveforms were determined by performing intensity cross-correlation measurements with 75 fs pulses directly out of the CPM laser (using second harmonic generation in the noncollinear geometry). Optical power spectra were monitored by directing the reconstructed beams to a 0.32 m spectrometer and an optical multichannel analyzer.

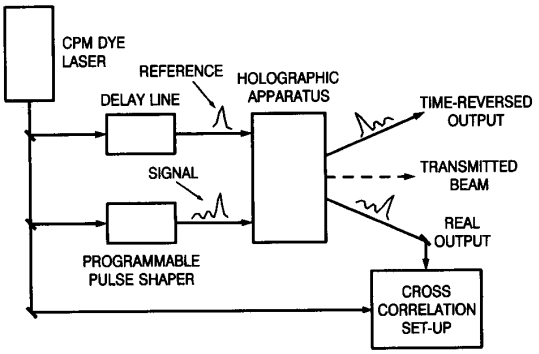

Fig. 2. Overall experimental apparatus.

III. Experimental Results

In this section we report on a series of several experiments showing femtosecond waveform processing by spectral holography. Our results demonstrate storage, recall, and time reversal of shaped pulses, as well as correlation and convolution of pairs of shaped waveforms. Furthermore, we demonstrate the use of spectral holography to perform matched filtering (an operation intimately related to pattern recognition) of femtosecond pulse waveforms. Finally, we present data indicating the ability to synthesize trains of femtosecond pulses by multiple exposures of the hologram.

A. Storage, Recall, and Time Reversal of Time-Delayed Pulses

As a first simple example, we describe the results of experiments in which signal pulses were not shaped but were delayed by various amounts with respect to the reference beam [30]. In separate measurements, spectral holograms were recorded for signal pulses delayed by 0, 1, and 2 ps, respectively, under stepper motor control. Fig. 3(a) shows real reconstructed pulses resulting when each of these spectral holograms is read out with a short test pulse with $\bar{k}_t = \bar{k}_r$. The pulse arrival times are identical to those of the original signal pulses. Fig. 3(b) shows

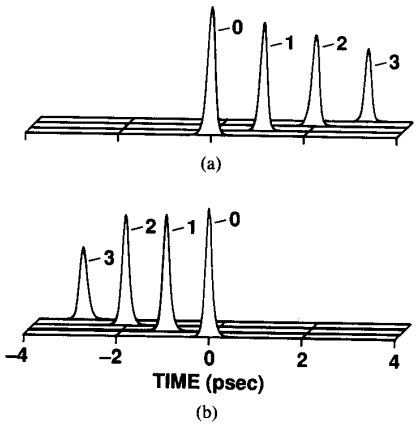

Fig. 3. Reconstructed waveforms from four separate spectral holograms. The holograms are recordings of short (unshaped) signal pulses delayed by 0, 1, 2 and 3 ps, respectively, as noted on the figure. (a) Real reconstructed pulses read out with $\bar{k}_t = \bar{k}_r$. (b) Time-reversed pulses read out with $\bar{k}_t = \bar{k}_s$.

measurements of time-reversed pulses obtained by reading out with short test pulses with $\bar{k}_t = \bar{k}_s$. The pulse arrival times are now opposite those of the original signal pulses. These data demonstrate the ability to record spectral holograms and to reconstruct real and as well as time-reversed replicas of the original signal.

The durations of the cross-correlation traces in Fig. 3 are on the order of 170 fs full width at half maximum (FWHM). Taking into account the 75 fs duration of the probe pulses employed in the cross-correlation measurement, this corresponds to a duration on the order of 150 fs FWHM for the reconstructed pulses. This modest broadening with respect to the input pulses can be understood on the basis of (1) and (2). Equation (1) shows that the reconstructed spectrum $E_{\text{out}}(\omega)$ is narrowed due to the multiplication of the test, reference, and signal spectral. Conversely, (2) predicts that the temporal duration of the output pulse will be broadened because of the convolution of test, reference, and signal pulses. For the case of Gaussian pulse shapes, the convolutions indicated in (2) would lead to broadening by a factor of $\sqrt{3}$, in rough agreement with the data. We remark that in some cases we were able to obtain shorter reconstructed pulses, ~ 120 fs in duration. Such variations in the reconstructed pulsewidths may result from different exposure conditions for holographic recording. For example, if the hologram is overexposed, the amplitude of fringes recorded at the peak of the optical spectrum saturates, and the spectral hologram is actually broadened. This would result in reconstructed pulses with an increased spectral width and hence with a narrower temporal duration.

We also note from Fig. 3 that the intensities of reconstructed pulses fall off for time delays of 2–3 ps. This occurs because signals which occupy a temporal window exceeding the inverse of the available spectral resolution cannot be effectively recorded. For our current setup with 600 line/mm gratings, the resolution is ~ 1 Å, corresponding to a temporal window of ~ 5 ps FWHM, in reasonable agreement with the data. Physically, the spectral resolution is set by the finite spot size of individual optical frequency components at the plane of the hologram and by the spectral dispersion $\delta x/\delta\lambda$; improved spectral resolution can be obtained by increasing the angular dispersion of the gratings and the input beam size. The spectral resolution available within a pulse shaping apparatus has been discussed in some detail in previous publications [5], [35].

In order to elucidate the way the signal pulse is stored as a spectral hologram, we digress to discuss the fringe patterns recorded for the delayed signal pulses of Fig. 3. We recall that if $e_s(t)$ and $E_s(\omega)$ are a Fourier transform pair, then the delayed signal $e_s(t-\tau)$ is the Fourier transform of $E_s(\omega)\exp(-i\omega\tau)$. Thus, a delay in the time domain corresponds to a phase shift which is linear with frequency and proportional to the delay. As a result, a delay in the signal pulse with respect to the reference pulse will cause a tilt in the fringe pattern at the hologram plane. In order to verify this point, we imaged fringe patterns corresponding to different signal pulse delays onto a CCD array and observed them on a monitor. Fig. 4 shows photographs of the display on the monitor for delays of 0, 6, and -6 ps. For zero delay ($\tau = 0$), the fringes are parallel with respect to the horizontal alignment line, and the fringe visibility is quite good. Note that the magnification is such that only a very small portion of the fringe pattern fits onto the photographs. The width of the photographs corresponds to 36 μm along the x direction of Fig. 1, equivalent to a spectral width of 1.2 Å. For $\tau = 6$ ps (middle photograph), a tilt in the fringe pattern is clearly evident. The amount of phase shift is roughly one half a fringe over the 1.2 Å bandwidth of the photograph. Since $\Delta\lambda = 1.2$ Å implies $\Delta\nu = 0.094$ THz, where $\nu = \omega/2\pi$ is the optical frequency, for a 6 ps delay we expect a shift equal to $\Delta\nu\tau = 0.56$ fringes, in good agreement with the data. For $\tau = -6$ ps, the fringes tilt by the same amount but in the opposite direction compared to the $\tau = 6$ ps photograph, again as expected. Also, we could clearly observe that the fringe visibility for $\tau = \pm 6$ ps was degraded compared to that for $\tau = 0$ (note that the fringe visibility could be more easily discerned from the real-time display than from the photographs reproduced in Fig. 4). The reduction in fringe visibility is expected, of course, because the 6 ps time delay exceeds the inverse of the available spectral resolution, or equivalently because the fringe pattern shifts appreciably within a bandwidth equal to the spectral resolution.

B. Storage, Recall, and Processing of Shaped Waveforms

We now demonstrate holographic storage and read out of a complex, shaped waveform [30]. As an example we consider a signal pulse distorted by a cubic spectral phase modulation. The signal pulse was shaped by using the liquid crystal phase modulator [32] in the auxiliary pulse shaper to generate a cubic spectral phase modulation of

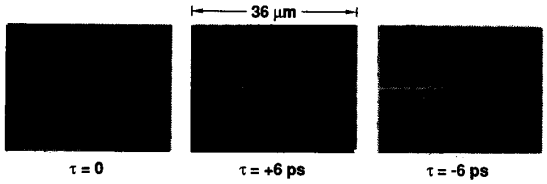

Fig. 4. Photographs of the interference pattern between spectrally dispersed signal and reference beams. The photos correspond to short (unshaped) pulses delayed by 0, 6, and −6 ps, respectively, with respect to the reference pulses. Note the tilt in the fringe pattern which arises for nonzero delay.

the form $\phi = -0.20(\nu - \nu_o)^3$. Here ϕ is the phase in radians, ν is the optical frequency in units of THz and ν_o is the center frequency. An intensity cross-correlation trace of the input signal pulse is plotted in Fig. 5(a). The spectral phase modulation leads to a complicated, nonsymmetric pulse distortion in the time domain. The most prominent effect is the appearance of long oscillatory tail; in addition, the main peak near $t = 0$ is slightly broadened, delayed and reduced in amplitude. Deviations from an exact cubic spectral phase dependence cause a slight irregularity in the shape and the depth of the oscillatory modulation. Distortion due to cubic phase variation is an important effect for ultrashort pulse propagation in optical fibers at the so-called zero dispersion wavelength, [36] for chirped-pulse amplification, [37] and for compression of femtosecond pulses to durations below 10 fs [38].

Fig. 5(b) and (c) shows intensity cross-correlation measurements of reconstructed pulses obtained by using $\bar{k}_t = \bar{k}_r$ and $\bar{k}_t = \bar{k}_s$, respectively. The test pulses were in both cases unshaped pulses ~75 fs in duration. As in the case of Fig. 3, the reconstructed pulses correspond to real and time-reversed replicas of the original distorted signal pulse, respectively. In the time-reversed case, the oscillatory tail appears *before* rather than *after* the main initial peak; furthermore, the main peak is found before $t = 0$ in the time-reversed data [Fig. 5(c)], whereas the main peak is slightly after $t = 0$ in the input signal [Fig. 5(a)] and in the real reconstructed output [Fig. 5(b)].

By using shaped test pulses, we can also demonstrate more complex signal processing operations. The second term in (2), proportional to $e_t(t) * e_r(t) * e_s(-t)$, corresponds in the time domain to the correlation of the test and signal waveforms, convolved with the reference. Since the reference is essentially an impulse function, the convolution has little effect; thus, the reconstructed waveform is essentially the temporal correlation between $e_t(t)$ and $e_s(t)$. Fig. 5(d) shows the reconstructed waveform in the $\bar{K}_2$ direction resulting when the test pulse is identical to the input signal pulse. In this case the quantity $E_t(\omega)E_s^*(\omega)$ is essentially unity, since $E_t(\omega)$ and $E_s(\omega)$ are modulated only in phase. The output waveform, which is the field autocorrelation of the signal waveform, is a short and featureless femtosecond pulse, without the distortion present in the input [Fig. 5(a)]. Furthermore, because all the energy now resides in a single pulse, the peak intensity in Fig. 5(d) is 60% higher than that of the real reconstructed pulse [Fig. 5(b)]. This result illustrates the use of spectral holography to generate matched filters for femtosecond pulse waveforms, a topic which we will discuss at greater length below.

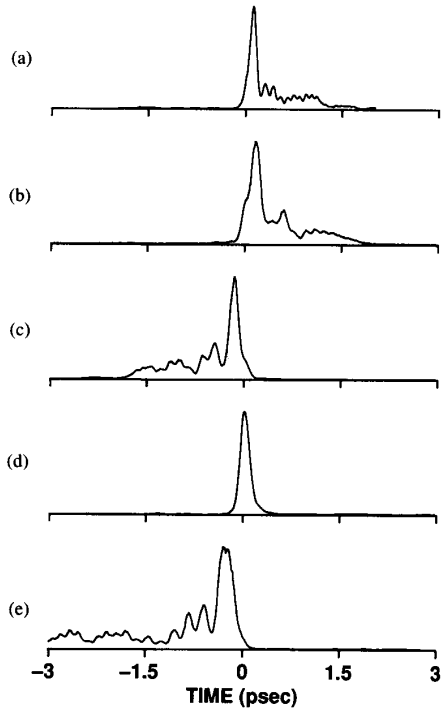

Fig. 5. Intensity cross-correlation measurements, showing holographic storage and recall of a signal pulse distorted via cubic spectral phase modulation. The curves are individually normalized for the same height. (a) Input signal pulse. (b) Real reconstructed output pulse ($\bar{k}_t = \bar{k}_r$). (c) Time-reversed output pulse ($\bar{k}_t = \bar{k}_s$). (d) Autocorrelation of the signal field, obtained using a test pulse identical to the signal pulse (with $\bar{k}_t = \bar{k}_s$). The peak is actually 1.6× stronger than that in (c). (e) Time-reversed autoconvolution of the signal field, obtained using a test pulse time-reversed with respect to the signal pulse (with $\bar{k}_t = \bar{k}_s$). The peak is actually 2× weaker than that in (c).

We can also demonstrate cross-correlations of nonidentical test and signal waveforms. Fig. 5(e) shows the output pulse which occurs when the liquid crystal modulator is reprogrammed so that the test pulse experiences a spectral phase modulation equal and opposite to that of the signal pulse. In this case the test waveform is itself a time-reversed version of the signal; therefore, the output in the $\bar{K}_2$ direction is the autoconvolution of a time-reversed version of the original signal waveform. The autoconvolution operation results in an effective cubic phase modulation twice as large as that on the original signal. The results are clearly evident in the data. The oscillatory tail now extends for longer than 3 ps, compared to ~1.5 ps for the original signal waveform, and the main pulse is broadened from ~150 to ~250 fs. Note that the ability to perform the convolution operation is intimately tied to the ability to generate time-reversed waveforms. Since time-reversal of ultrashort waveforms cannot be per-

formed using the standard techniques of ultrafast optics, neither can convolution operations. Holographic techniques, such as the one reported here, are to our knowledge the only means for performing time-reversal and convolution operations on ultrashort optical pulses.

C. Matched Filtering of Femtosecond Waveforms

Matched filtering is a powerful signal processing operation with applications to pattern recognition and pulse compression. One well known example in optics is the VanderLugt correlator, [39] which compares a two-dimensional spatial image with a desired target, by passing the input image through a filter matched to the target. Matched filtering is also an integral part of chirped radar and fiber-and-grating optical pulse compression; in both cases all the energy in a long, frequency-swept input pulse is compressed by the matched filter into a short and intense, transform-limited output pulse. Below we discuss the use of spectral holography to generate matched filters for femtosecond optical waveforms. Examples include decoding of low intensity, phase-coded pseudonoise bursts into intense femtosecond pulses and recovery of femtosecond waveforms stored in an encrypted format.

1) Encoding and decoding of femtosecond pulses: We previously demonstrated spectral phase coding and decoding of femtosecond pulses by using fixed, microlithographically fabricated masks [3]–[5]. Encoding was achieved by placing a pseudorandom binary phase mask at the filtering plane of a pulse shaping apparatus. By scrambling the phases of the various frequency components contained within the incident femtosecond pulse, the mask converted the incident pulse into a low intensity, picosecond-duration, pseudonoise burst. Decoding was achieved by using a second prefabricated mask (constituting a phase conjugate or matched filter for the first) to unscramble the spectral phases and restore the original pulse. The intensity contrast between such coded and decoded pulses has been proposed as the basis for a code-division multiple-access optical communications network [3], [6].

We have now demonstrated the use of spectral holography to produce matched filters for incoming femtosecond waveforms. Encoded signal pulses were first generated by using a pseudorandom phase mask patterned according to a length-31 M-sequence [40], and a spectral hologram of the encoded signal pulse was then recorded. Matched filtering operation was demonstrated by reading out the spectral hologram with various test waveforms (using $\bar{k}_t = \bar{k}_s$ and looking in the $\bar{K}_2$ direction). Typical data are shown in Fig. 6. Figure 6(a) shows the 2 ps pseudonoise burst which results when the spectral hologram is read out by using an unshaped test pulse, and Fig. 6(b) shows the decoded pulse which results when the test waveform is the same as the original signal. In the latter case the test is recompressed by the spectral hologram into a featureless, ~100 fs pulse, with a quite obvious increase in intensity. Both the duration and the intensity of

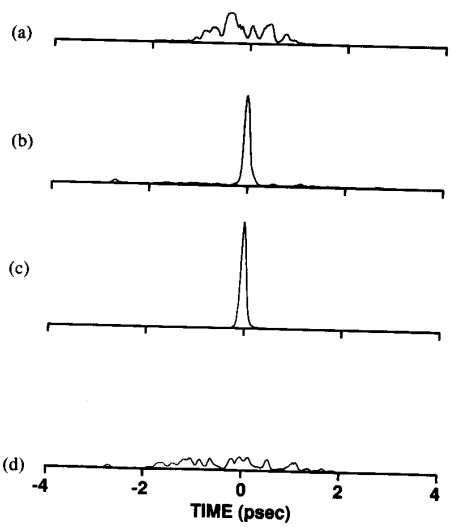

Fig. 6. Intensity cross-correlation measurements of encoded and decoded pulses. These traces are obtained by using various test pulses to read out the spectral hologram of a signal pulse encoded using a pseudorandom phase mask. The output is examined in the $\bar{K}_2$ direction. (a) Encoded pulse read out by using an unshaped test pulse. (b) Decoded pulse read out by using a test waveform identical to the original signal waveform. (c) Pulse resulting when signal, test, and reference beams are all short (unshaped) femtosecond pulses, plotted for comparison with (b). (d) Output waveform resulting when the original spectral hologram is read out with a coded test waveform different than the original coded signal beam. In this case decoding is not achieved.

the recompressed pulse are comparable to that obtained when signal and test beams are both unshaped fsec pulses [plotted for reference in Fig. 6(c)]. The recompressed pulse does exhibit some residual energy in the wings, which may result due to nonlinearity and/or nonuniformity in the process of recording the spectral hologram and due to spurious amplitude modulation which occurs when phase jumps occur within a bandwidth smaller than the spectral resolution [35] of the shaping apparatus. Finally, Fig. 6(d) shows the output waveform obtained when the original spectral hologram is read out with a coded test waveform different than the original signal waveform (the mask used for coding was slightly repositioned within the optical spectrum, by one mask pixel, before read out). The waveform is once again a low intensity pseudonoise burst, demonstrating that no strong correlation peak results when the input waveform is not matched to the filter.

The data above are similar to those obtained previously by using fixed phase masks [3], [5]. There are however several differences. First, in order to simplify the setup, in previous experiments coding and decoding masks were placed back to back within a single pulse shaping apparatus. In the current work, in which coding and decoding are performed in separate shaping apparata, the results more realistically demonstrate true matched filtering. Second, and more importantly, holographic decoding (as well as other holographic signal processing operations) is self-aligned. Unlike the case of fixed masks, for which the spectral dispersion of the two pulse shapers and the po-

sitions of the coding and decoding masks would have to be precisely matched, the holographic pulse shaper automatically produces a spectral hologram matched to the incoming signal. Finally, although not demonstrated in the current experiments, we note the possibility of storing multiple matched filters within the same spectral hologram by means of angular multiplexing. In that scenario different waveforms could be stored by varying the fringe period (in the y direction). This would allow simultaneous correlation of an incoming waveform with multiple stored templates; each correlation would correspond to a different diffracted direction.

2) Storage and read out of encrypted femtosecond waveforms: We have also performed experiments demonstrating the ability to store encrypted femtosecond waveforms and subsequently to recover the original, unscrambled data. Consider a signal field with a spectrum given by $E_s(\omega) = E_{\text{data}}(\omega)E_{\text{noise}}(\omega)$, where $E_{\text{data}}(\omega)$ and $E_{\text{noise}}(\omega)$ correspond to the desired waveform and a pseudorandom phase code, respectively. The data waveform can be recovered from a spectral hologram of $E_s(\omega)$ by using a test field given by $E_t(\omega) = E_{\text{noise}}(\omega)$. In that case the waveform read out from the hologram in the $\overline{K}_2$ direction (assuming a short reference pulse with a broad spectrum) is $E_{\text{out}}(\omega) \sim E_{\text{data}}(\omega)|E_{\text{noise}}(\omega)|^2$, which reduces to $E_{\text{data}}(\omega)$ if the encrypting field $E_{\text{noise}}(\omega)$ is purely phase modulated. On the other hand, if the encrypting field is not known, the data waveform cannot be recovered.

We have demonstrated this concept as follows. Two separate phase masks were placed within the pulse shaper used for generating the signal beam. One, which corresponds to $E_{\text{noise}}(\omega)$, contains the same length-31 M-sequence, pseudorandom phase mask used in Section III-C-1. The second mask, corresponding to $E_{\text{data}}(\omega)$, contains a π phase shift at the center of the spectrum but is otherwise featureless. In the time domain the data mask alone generates a pulse doublet with a null at $t = 0$ [see Fig. 7(a)]; this waveform is termed an "odd pulse" because the field is antisymmetric in time [2], [5]. A spectral hologram corresponding to $E_{\text{data}}(\omega)E_{\text{noise}}(\omega)$ is recorded and then read out with various test waveforms. When the test waveform is identical to the encrypting waveform ($E_t(\omega) = E_{\text{noise}}(\omega)$), the odd pulse is recovered [Fig. 7(b)]. On the other hand, when the test beam is either an unshaped pulse [Fig. 7(c)] or a shifted version of $E_{\text{noise}}(\omega)$ [Fig. 7(d)], the odd pulse is totally obscured. These data demonstrate holographic storage of femtosecond waveforms in a scrambled format. Retrieval of the original waveform can be accomplished only with knowledge of the code used for scrambling.

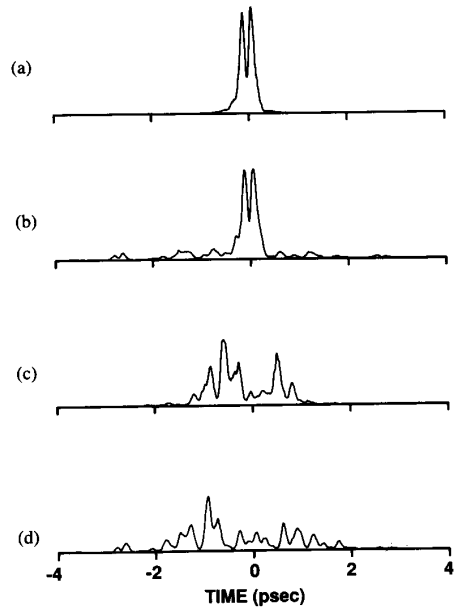

Fig. 7. Intensity cross-correlation measurements showing storage and recall of encrypted femtosecond waveforms. The spectral hologram contains the product of the desired spectral data and a pseudorandom spectral code used for encryption. Data are read out in the $\overline{K}_2$ direction. (a) Measurement of a femtosecond "odd" pulse, corresponding to the desired data. No encrypting code was used. (b) Waveform resulting when the encrypted spectral hologram is read out with a test pulse identical to the encrypting spectral code. The stored data are recovered. (c) Read out with a short, unshaped test pulse. The desired data are scrambled. (d) Read out with a test pulse corresponding to a shifted version of the encrypting code. Again, the data are obscured.

D. Waveform Synthesis by Spectral Holography

Another application of spectral holography is for synthesizing desired femtosecond waveforms or pulse trains. The idea is to use spectral holography as a means of recording a linear filter which will reshape a known input pulse into the desired output waveform. This could be used either to store and replicate an existing femtosecond waveform and its corresponding pulse shaping filter (as in Sections III-A and B) or as a convenient means to generate a new filter for a pulse shape not previously available.

Let us compare our standard pulse shaping technique [5] with pulse shaping via spectral holography. Within some broad limits, a standard pulse shaping setup using spatially patterned masks is sufficient to generate any desired pulse shape, provided that gray-level control of both the spectral amplitudes and the spectral phases is available. This can and has been achieved by careful patterning of partially opaque metal films for gray-level amplitude masks [5], [41] or by utilizing a multielement phase modulator for gray-level phase control [31], [32]. However, in some cases the desired waveform in the time domain may be much simpler than the corresponding amplitude and phase spectra in the frequency domain. For example, a pulse train composed of pulses with identical amplitudes and phases but different pulsewidths and spacings would appear rather simple in the time domain but would require precise gray-level control of both phase and amplitude in the frequency domain. In such cases it may be advantageous to utilize holography, which automatically provides gray-level control, to record the required mask.

Mazurenko [29] has proposed that holograms of spatially patterned, monochromatic laser beams can be used as pulse shaping masks within a pulse shaping apparatus, and Ema and Shimizu [14] have demonstrated this approach in experiments performed on a picosecond time scale. The idea is to use a transparency with a spatial pattern equal to a scaled version of the desired temporal pattern. A Fourier transform hologram of the mask is recorded with a cw laser and then placed into a pulse shaping apparatus. The hologram shapes the spectrum of the read out pulse according to the Fourier transform of the spatial pattern on the transparency. As a result, the temporal waveform of the pulse emerging from the shaper is a scaled version of the spatial pattern on the transparency.

We propose a different approach in which the holographic material is placed within a pulse shaping apparatus from the outset. Multiple-pulse trains or other waveforms can be formed by multiple exposures of the holographic recording material. In order to synthesize the spectral hologram of a pulse train, for example, a separate exposure would be made for each pulse in the desired pulse train. The signal could be an unshaped, short pulse identical to the reference; the delay of the signal pulse would be adjusted separately for each exposure according to the desired delay in the final pulse train. More complicated pulse trains or waveforms could be built up by using shaped signal pulses, which could be changed from one exposure to the next.

We have performed experiments testing this technique. For each exposure the signal pulse delay was first set by using a stepper motor; a shutter was then opened for a duration of 4 ms in order to expose the thermoplastic plate to signal and reference beams. No attempt was made to control the relative phases of the signal pulses at different delays, although in principle this could be achieved, e.g., by using techniques introduced by Scherer *et al.* [15] to produce phase-locked pulse pairs. Fig. 8(a) and (b) show some typical data, which are read out in the $\overline{K}_1$ direction. These traces are intensity cross-correlation measurements of three-pulse bursts, read out from spectral holograms produced using three exposures with signal pulse delays of 0, 0.5, and -1 ps. The first trace shows three clean pulses at the desired positions and with nearly equal amplitudes. The second trace, which was obtained from a second experimental run, shows the same three pulses at the same desired positions, but this time with quite different amplitudes. Another example of our data, Fig. 8(c), shows the possibility of synthesizing longer pulse trains. Exposures were made at signal delays of 0, 1, 1.5, 2, -0.5, and -2 ps; each of these six pulses are evident in the data read out from the final hologram, although the amplitudes again vary by a great deal.

In general, we found strong variations in the amplitudes of pulses within a train, although all the pulses expected were present. Furthermore, the relative amplitudes of the various pulses varied from one experimental run to the next, as shown by Fig. 8(a) and (b). These variations may arise due to the lack of control of the relative phases at different signal pulse delays (these phase variations would not be expected to be reproducible from one experimental run to the next), together with saturation effects in the hologram. The several pulses present in the time domain will interfere in the frequency domain to produce a structured spectrum with various peaks and minima. Variations in the temporal phases will cause the spectral structure to change as well. Saturation of the hologram, due to overexposure or limited dynamic range, can clip the peaks in the spectral structure and lead to the observed amplitude variations in the time domain. In order to achieve better experimental precision, the phases of the signal pulses should be controlled, and care should be exercised to achieve linear recording.

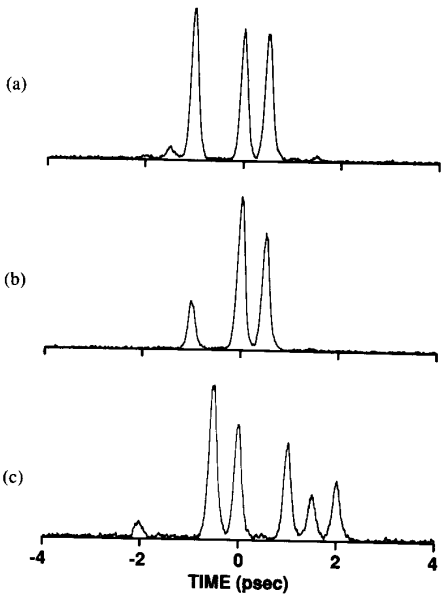

Fig. 8. Femtosecond waveform synthesis. The plots are intensity cross-correlation traces obtained by reading out ($\overline{K}_1$ direction) spectral holograms recorded using multiple exposures. (a) and (b) Two experimental trials for multiple exposures corresponding to signal pulse delays of 0, 0.5, and -1 ps. (c) Waveform resulting for multiple exposures with signal pulse delays at 0, 1, 1.5, 2, -0.5, and -2 ps.

IV. Discussion and Further Applications

It is worth contrasting our spectral holography experiments to related works by other authors. As noted in the introduction, several groups have reported on the use of spectral hole burning and photon echoes in inhomogeneously broadened resonant absorbers to perform spectral holography [20]–[26]. Mathematically there is a close analogy between the technique reported here and that using inhomogeneously broadened absorbers. One difference involves causality: the amplitude and phase of holes burned within inhomogeneously broadened lines must satisfy the Kramers–Kronig relation; this implies that photon echoes read out from such spectral holograms can occur only *after* the read out pulse. In the present paper

there is no such restriction: the phases and amplitudes in the spectral domain can be set independently; therefore, the reconstructed output pulse can emerge from the setup *before* the transmitted read out pulse! There is no violation of causality, of course, due to the intrinsic delay associated with the spectral holography setup itself. A second difference is related to temporal resolution. The present technique has been demonstrated on a 100 fs time scale and could readily be extended to a faster time scale by using shorter pulses. On the other hand, spectral holography using resonant absorbers is usually limited by available inhomogeneous linewidths to time scales of 100 fs or longer. Finally, the current technique is essentially independent of wavelength, while spectral hole burning and photon echoes require a match between the laser and absorber. On the other hand, spectral holography in inhomogeneous absorbers makes available four dimensions for signal processing (frequency plus three spatial axes), whereas at most three dimensions (frequency plus two independent spatial axes) are available from spectral holography within a pulse shaping apparatus.

Recently, Da Silva *et al.* [42] have reported a "noncausal photon echo" experiment rather closely related to our implementation of spectral holography. In their work a collinear pulse pair is directed into a pulse shaping apparatus containing a medium with thermal nonlinearity at the filter plane. As a result of the nonlinearity, echo pulses are produced both before and after the incident pulse pair. Their experiment is analogous to on-axis Fourier-transform holography, while the work reported by us is analogous to off-axis Fourier transform holography.

We also comment on the relation of our current work to linear and nonlinear spectral filtering. As noted earlier, nonlinear filtering is required to achieve operations such as time reversal or correlations between two independent waveforms. In our paper the final output pulses result from the interaction of three independent waveforms; time reversal, correlations, or convolutions can be performed without *a priori* knowledge of the inputs. In this sense our experiments are an example of nonlinear filtering. On the other hand, the recording phase of our experimental procedure may be regarded as a way to generate a fixed, linear mask containing information related to signal and reference beams. During the read out phase, this fixed mask acts as a linear filter operating on the test beam. This ambiguity between linear and nonlinear filtering operations would be resolved by replacing the thermoplastic plate with a *real-time* (as opposed to *sequential*) holographic medium, such as a photorefractive crystal, or even a medium with thermal nonlinearity.

In addition to the applications discussed in Section III, ultrashort pulse spectral holography may have several additional applications, including measurement of ultrashort pulse shapes, parallel-to-serial conversion, and dispersion compensation. These examples are discussed below.

a) Measurement of intensity profiles: Measurements of ultrashort optical pulses are typically performed by the second harmonic generation technique. This yields the intensity autocorrelation function, which is not sufficient to determine the exact pulse shape. On the other hand, the pulse shape can in principle be derived from knowledge of the intensity *autoconvolution*. Measurement of the intensity autoconvolution function requires availability of both a real and a time-reversed version of the waveform to be measured. The setup is the same as that used for second harmonic generation autocorrelation measurements, except that one real and one time-reversed waveform are used as the input. As we have shown, time reversal can be achieved via holographic processing; therefore, the autoconvolution technique could be implemented for measurement of femtosecond intensity profiles.

b) Parallel-to-serial conversion: Our previous work on femtosecond pulse shaping and this current paper on femtosecond spectral holography involve a natural mapping of the optical frequency axis onto a single spatial dimension. In essence, a parallel modulation in the spatial domain is transferred onto the frequency spectrum, and this corresponds to an ultrafast serial modulation in the time domain. Thus, pulse shaping or spectral holography can be used for conversion of a parallel spatial signal into a serial temporal signal.

c) Dispersion compensation: One very interesting potential application of spectral holography is for dispersion compensation. We have seen that spectral holography can be used to generate matched filters which cancel the phase variation of incoming pulses, thus compressing chirped pulses to the bandwidth limit. A possible experimental setup is sketched in Fig. 9. A modulated stream of femtosecond pulses is transmitted through an optical fiber. The power is kept sufficiently low that nonlinear effects in the fiber are not important. At the output of the fiber, the pulses are broadened due to group velocity dispersion. These pulses are then input as the signal beam into a spectral holography apparatus. A mode-locked local oscillator provides a synchronized train of bandwidth-limited femtosecond pulses (synchronized to the incoming data stream) for the reference beam. The interference between signal and reference beams forms a spectral hologram of the phase variations imposed by the dispersive transmission channel. Subsequent passage of the dispersed pulses through the holography apparatus cancels their chirp and restores the original femtosecond data stream. The feasibility of such chirp compensation was demonstrated in Fig. 5(d), which showed restoration of a pulse distorted by a cubic phase variation. The spectral hologram can be recorded permanently, as in the current experiments, in order to compensate for a fixed dispersion, or can be updated in real time (using a real-time holographic recording material) in order to adaptively compensate a time-varying dispersion. One advantage of this approach is that the phase variation need not be known *a priori* since the holographic process automatically produces a matched filter corresponding to the incoming phase variation. Possible applications include not only fiber dispersion compensation, but also chirped pulse am-

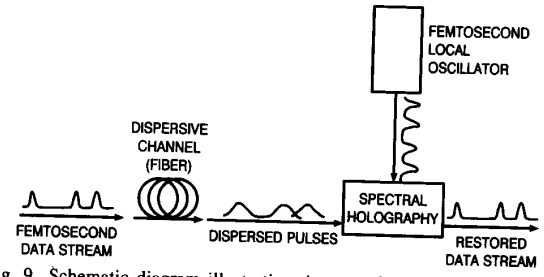

Fig. 9. Schematic diagram illustrating the use of spectral holography to compensate for dispersion in fibers. The holographic process automatically produces a matched filter corresponding to the phase variation on the dispersed pulses.

plification [37] and compression of very short (<10 fs) pulses where cubic and possibly higher order phase variations are important [38], [43]. In order to compensate for fiber dispersion between remote sites, one difficulty which much be overcome is the need for a synchronized femtosecond local oscillator. This same issue also arises in all-optical switching schemes based on high-speed, synchronous logic gates implemented using soliton trapping and soliton dragging effects [44].

V. Conclusion

In summary, we have demonstrated frequency domain holographic processing of femtosecond light pulses. Our experiments were implemented by using a modified femtosecond pulse shaping apparatus with a holographic recording medium inserted at the filter plane. In the current paper we have used a thermoplastic plate as a thin holographic medium. The interference pattern between spectrally dispersed reference and signal waveforms is first recorded; the resulting spectral hologram is subsequently read out by a test waveform. For a test beam consisting of a short pulse with a uniform spectrum, read out results in reconstruction of a real or time-reversed version of the original signal beam (depending on the geometry). Read out of the hologram with a spectrally patterned, temporally shaped test pulse yields an output waveform which is either the correlation or the convolution of the test field with the signal field (again depending on the geometry). To date, holography is the only way to perform signal processing operations such as time-reversal, correlation, and convolution on ultrashort light pulses. Our work extends well-known principles of holographic processing, used extensively for pattern recognition and filtering of two-dimensional spatial signals, to the femtosecond time domain.

In addition, we have presented several further applications of femtosecond spectral holography. Perhaps the most important of these is matched filtering. Matched filtering can be used for encoding and decoding of ultrashort pulses for high-speed information networking, for compensation of fiber dispersion, and for femtosecond pulse compression. We have also demonstrated storage and recall of encrypted waveforms which can be replayed only with knowledge of the waveform used for encrypting. Finally, we have discussed the use of spectral holography to produce pulse shaping masks for femtosecond waveform synthesis.

For the future it will be important to extend our experiments to the 1.3 and 1.5 μm wavelength ranges most suitable for fiber transmission and optical communications. This will require identification of a suitable holographic material sensitive to these wavelengths. By utilizing real-time media, such as photorefractives or other nonlinear materials, it will be possible to adaptively reconfigure the spectral hologram in response to changing signal or reference beams. Furthermore, by including feedback from the diffracted output beams back to the input, it may be possible to achieve associative recall of ultrashort pulse waveforms, in close analogy with optical implementations of associative memories and neural networks in the spatial domain. This could permit reconstruction of an entire femtosecond waveform in response to a partial input, perhaps with error correction capability.

Acknowledgment

The authors gratefully acknowledge engaging discussions with Y. Silberberg.

References

[1] C. Froehly, B. Colombeau, and M. Vampouille, "Shaping and analysis of picosecond light pulses," in *Progress in Optics*, E. Wolf, Ed. Amsterdam: North-Holland, 1983, vol. 20, pp. 115–121.

[2] J. P. Heritage, A. M. Weiner, and R. N. Thurston, "Picosecond pulse shaping by spectral phase and amplitude manipulation," *Opt. Lett.*, vol. 10, p. 609, 1985.

[3] A. M. Weiner, J. P. Heritage, and J. A. Salehi, "Encoding and decoding of femtosecond pulses," *Opt. Lett.*, vol. 13, p. 300, 1988.

[4] A. M. Weiner and J. P. Heritage, "Picosecond and femtosecond Fourier pulse shape synthesis," *Revue Phys. Appl.*, vol. 22, p. 1619, 1987.

[5] A. M. Weiner, J. P. Heritage, and E. M. Kirschner, "High-resolution femtosecond pulse shaping," *J. Opt. Soc. Amer. B* vol. 5, p. 1563, 1988.

[6] J. A. Salehi, A. M. Weiner, and J. P. Heritage, "Coherent ultrashort light pulse code-division multiple access communication systems," *J. Lightwave Tech.*, vol. 8, p. 478, 1990.

[7] A. M. Weiner, J. P. Heritage, R. J. Hawkins, R. N. Thurston, E. M. Kirschner, D. E. Leaird, and W. J. Tomlinson, "Experimental observation of the fundamental dark soliton in optical fibers," *Phys. Rev. Lett.*, vol. 61, p. 2445, 1988; A. M. Weiner, R. N. Thurston, W. J. Tomlinson, J. P. Heritage, D. E. Leaird, E. M. Kirschner, and R. J. Hawkins, "Temporal and spectral self-shifts of dark optical solitons," *Opt. Lett.*, vol. 14, p. 868, 1989.

[8] A. M. Weiner, Y. Silberberg, H. Fouckhardt, D. E. Leaird, M. A. Saifi, M. J. Andrejco, and P. W. Smith, "Use of femtosecond square pulses to avoid pulse breakup in all-optical switching," *IEEE J. Quantum Electron.* vol. 25, p. 2648, 1989.

[9] J. P. Heritage, E. W. Chase, R. N. Thurston, and M. Stern, "A simple femtosecond optical third-order disperser," presented at CLEO, Baltimore, MD, 1991; P. J. Delfyett, J. P. Heritage, E. W. Chase, and R. N. Thurston, "Femtosecond pulse generation by cubic phase compensation in semiconductor traveling wave amplifiers," presented at CLEO, Baltimore, MD, 1991.

[10] J. L. A. Chilla and O. E. Martinez, "Direct determination of the amplitude and the phase of femtosecond light pulses," *Opt. Lett.*, vol. 16, p. 39, 1991.

[11] A. M. Weiner, D. E. Leaird, G. P. Wiederrecht, and K. A. Nelson, "Femtosecond pulse sequences used for optical control of molecular motion," *Science*, vol. 247, p. 1317, 1990; A. M. Weiner, D. E. Leaird, G. P. Wiederrecht, and K. A. Nelson, "Femtosecond mul-

tiple-pulse impulsive stimulated Raman scattering spectroscopy," *J. Opt. Soc. Amer. B*, vol. 8, p. 1264, 1991.
[12] M. Haner and W. S. Warren, "Generation of programmable, picosecond-resolution shaped laser pulses by fiber-grating pulse compression," *Opt. Lett.*, vol. 12, p. 398, 1987; M. Haner and W. S. Warren, "Generation of arbitrarily shaped picosecond optical pulses using an integrated electro-optic waveguide modulator," *Appl Phys. Lett.*, vol. 52, p. 1458, 1988.
[13] T. Kobayashi and A. Morimoto, "Electro-optical synthesis of picosecond optical pulses," in *OSA Proceedings on Picosecond Electronics and Optoelectronics*, T. C. L. G. Sollner and D. M. Bloom, Eds. Washington, DC: OSA, 1989, p. 81.
[14] K. Ema and F. Shimizu, "Optical pulse shaping using a Fourier-transformed hologram," *Japan. J. Appl. Phys.*, vol. 29, p. 1631, 1990.
[15] N. F. Scherer, R. J. Carlson, A. Matro, M. Du, A. J. Ruggiero, V. Romero-Rochin, J. A. Cina, G. R. Fleming, and S. A. Rice, "Flourescence-detected wave packet interferometry: Time resolved molecular spectroscopy with sequences of femtosecond phase-locked pulses," *J. Chem. Phys.*, vol. 95, p. 1487, 1991.
[16] D. H. Reitze, A. M. Weiner, and D. E. Leaird, "Shaping of wide bandwidth 20 fsec optical pulses," *Appl. Phys. Lett.*, in press.
[17] W. S. Warren, "Effects of pulse shaping in laser spectroscopy and nuclear magnetic resonance," *Science*, vol. 242, p. 878, 1988.
[18] R. Collier, C. B. Burckhardt, and L. H. Lin, *Optical Holography*. Orlando, FL: Academic, 1977.
[19] D. A. B. Miller, "Time reversal of optical pulses by four-wave mixing," *Opt. Lett.*, vol. 5, p. 300, 1980.
[20] N. W. Carlson, L. J. Rothberg, A. G. Yodh, W. R. Babbitt, and T. W. Mossberg, "Storage and time reversal of light pulses using photon echoes," *Opt. Lett.*, vol. 8, p. 483, 1983; W. R. Babbitt and T. W. Mossberg, "Time-domain frequency-selective optical data storage in a solid-state material," *Opt. Commun.*, vol. 65, p. 185, 1988.
[21] M. K. Kim and R. Kachru, "Multiple-bit long-term data storage by backward-simulated echo in $Eu^{3+}:YAlO_3$," *Opt. Lett.*, vol. 14, p. 423, 1989.
[22] P. Saari, R. Kaarli, and A. Rebane, "Picosecond time- and space-domain holography by photochemical hole burning," *J. Opt. Soc. Amer. B*, vol. 3, p. 527, 1986.
[23] A. Rebane, J. Aaviksoo, and J. Kuhl, "Storage and time reversal of femtosecond light signals via persistent spectral hole burning holography," *Appl. Phys. Lett.*, vol. 54, p. 93, 1989.
[24] V. L. Da Silva, Y. Silberberg, J. P. Heritage, E. W. Chase, M. A. Saifi, and M. J. Andrejco, "Femtosecond accumulated photon-echo in Er-doped fibers," *Opt. Lett.*, vol. 16, p. 1340, 1991.
[25] M. Mitsunaga, R. Yano, and N. Uesugi, "Time- and frequency-domain hybrid optical storage," *Opt. Lett.*, vol. 16, p. 1890, 1991.
[26] Y. Silberberg, V. L. da Silva, J. P. Heritage, E. W. Chase, and M. J. Andrejco, "Accumulated photon-echoes in doped fibers," *IEEE J. Quantum Electron*, this issue, pp. 2369–2381.
[27] J. A. Valdmanis, H. Chen. E. N. Leith, Y. Chen, J. L. Lopez, N. H. Abramson, and D. S. Dilworth, "Three-dimensional imaging with femtosecond optical pulses," in *Conf. Lasers Electro-opt.*, vol. 7, 1990 OSA Tech. Dig. Ser. Washington, DC: OSA, 1990, p. 54.
[28] L. H. Acioli, M. Ulman, E. P. Ippen, J. G. Fujimoto, H. Kong, B. S. Chen, and M. Cronin-Golomb, "Femtosecond temporal encoding in barium titanate," *Opt. Lett.*, vol. 16, p. 1984, 1991.
[29] Y. T. Mazurenko. "Holography of wave packets," *Appl. Phys. B*, vol. 50, p. 101, 1990.
[30] A. M. Weiner, D. E. Leaird, D. H. Reitze, and E. G. Paek, "Spectral holography of shaped femtosecond pulses," *Opt. Lett.*, vol. 17, p. 224, 1992.
[31] A. M. Weiner, D. E. Leaird, J. S. Patel, and J. R. Wullert, "Programmable femtosecond pulse shaping by use of a multielement liquid-crystal phase modulator," *Opt. Lett.*, vol. 15, p. 326, 1990.
[32] ——"Programmable shaping of femtosecond optical pulses by use of a 128-element liquid crystal phase modulator," *IEEE J. Quantum Electron.*, vol. 28, pp. 908–919, Apr. 1992.
[33] J. A. Valdmanis, R. L. Fork, and J. P. Gordon, "Generation of optical pulses as short as 27 femtoseconds directly from a laser balancing self-phase modulation, group-velocity dispersion, saturable absorption, and saturable gain," *Opt. Lett.*, vol. 10, p. 131, 1985.
[34] S. D. Smith, *Holograhpic Recording Materials*. New York: Springer Verlag, 1977.
[35] R. N. Thurston, J. P. Heritage, A. M. Weiner, and W. J. Tomlinson, "Analysis of picosecond pulse shape synthesis by spatial masking in a grating pulse compressor," *IEEE J. Quantum Electron.*, vol. QE-22, p. 682, 1986.
[36] A. Frenkel, J. P. Heritage, and M. Stern, "Compensation of dispersion in optical fibers for the 1.3–1.6 μm region with a grating and telescope," *IEEE J. Quantum Electron.*, vol. 25, p. 1981, 1989; M. Stern, J. P. Heritage, and E. W. Chase, "Grating compensation of third-order fiber dispersion," *IEEE J. Quantum Electron.*, to be published, Dec. 1992.
[37] P. Maine, D. Strickland, P. Bado, M. Pessot, and G. Mourou, "Generation of ultrahigh peak power pulses by chirped pulse amplification," *IEEE J. Quantum Electron.*, vol. 24, p. 398, 1988.
[38] R. L. Fork, C. H. Brito Cruz, P. C. Becker, and C. V. Shank, "Compression of optical pulses to six femtoseconds by using cubic phase compensation," *Opt. Lett.*, vol. 12, p. 483, 1987.
[39] A. VanderLugt, "Signal detection by complex spatial filtering," *IEEE Trans. Inform. Theory.*, vol IT-10, p. 139, 1964.
[40] R. Skaug and J. F. Hjelmstad, *Spread Spectrum in Communications*. London: Peregrinus, 1985.
[41] A. M. Weiner, J. P. Heritage, and R. N. Thurston, "Synthesis of phase coherent picosecond optical square pulses," *Opt. Lett.*, vol. 11, p. 153, 1986.
[42] V. L. Da Silva and Y. Silberberg, "Noncausal photon echo," presented at Quantum Electron. Laser Conf., Anaheim, CA, May 10–15, 1992.
[43] C. H. Brito-Cruz, P. C. Becker, R. L. Fork, and C. V. Shank, "Phase correction of femtosecond optical pulses using a combination of prisms and gratings," *Opt. Lett.*, vol. 13, p. 123, 1988.
[44] N. M. Islam, C. E. Soccolich, and D. A. B. Miller, "Low-energy ultrafast fiber soliton logic gates," *Opt. Lett.*, vol. 15, p. 909, 1990; M. N. Islam, "Ultrafast all-optical logic gates based on soliton trapping in fibers," *Opt. Lett.*, vol. 14, p. 1257, 1989.

Andrew M. Weiner (S'84–M'84–SM'91), for a photograph and biography, see p. 919 of the April 1992 issue of this JOURNAL.

Daniel E. Leaird, For a photograph and biography, see p. 919 of the April 1992 issue of this JOURNAL.

David H. Reitze was born in Pittsburgh, PA, in 1961. He received the B.A. degree in physics from Northwestern University in 1983 and the Ph.D. degree in physics from the University of Texas at Austin in 1990 for studies of femtosecond dynamics of solid-liquid laser-induced phase transitions in carbon and silicon and for studies of two-photon absorption in silicon at above band-gap frequencies using femtosecond optical pulses. For this research, he was awarded a 1991 Outstanding Dissertation Prize from the University of Texas.

Since 1990, he has been employed as a post-doctoral member of the Technical Staff at Belcore in Red Bank, NJ. His current research centers around the development of ultrafast optical techniques, including high energy pulse compression, femtosecond pulse shaping, and spectral holography of femtosecond waveforms, as well as on ultrafast spectroscopy of high temperature superconductors.

Dr. Reitze is a member of Phi Beta Kappa, the Optical Society of America and the American Physical Society.

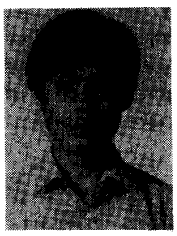

Eung Gi Paek received the B.Sc. degree in physics from Seoul National University in 1972 and the M.Sc. and Ph.D. degrees in physics from the Korea Advanced Institute of Science and Technology in 1976 and 1979, respectively.

From 1979 to 1981, he was with the Agency for Defense Development in Korea. In April 1982, he joined the California Institute of Technology, Pasadena, as a post-Doctoral Fellow and later as a Senior Research Fellow for a period of five years. Since May 1987, he has been with Bell Communications Research as a member of the Technical Staff. His current research interests are in the areas of optical computing, neural networks, hybrid optical signal-image processing, and pattern recognition, optical interconnects, and holographic memory.